

# Insights into the Structure and Surface Geology of Isla Socorro, Mexico, from Airborne Magnetic and Gamma-Ray Surveys

V. Paoletti<sup>1</sup> · S. Gruber<sup>2</sup> · N. Varley<sup>3</sup> · M. D'Antonio<sup>1</sup> ·  
R. Supper<sup>2</sup> · K. Motschka<sup>2</sup>

Received: 9 July 2015 / Accepted: 24 November 2015 / Published online: 14 December 2015  
© Springer Science+Business Media Dordrecht 2015

**Abstract** The island of Socorro is located in the eastern Pacific Ocean, 650 km off the coast of Mexico. It is a rare example of an oceanic volcanic island whose above sea level volume is made up mostly of peralkaline trachytes and rhyolites, with subordinate mafic rocks. Subaerial volcanism started several hundred thousand years ago and continues until recent times. We present an investigation of surface and subsurface geology of the island, based on the first detailed extensive geophysical survey on the island. Acquired airborne magnetic and gamma-ray data were compared to existing geological information and supplemented with field investigations and satellite imagery. Magnetic data show a wide minimum in the central part of the island, possibly connected to a high-temperature zone in the deeper central portion of the volcano, likely to be due to a still hot magma body. The data also depict two parallel edges possibly suggesting the existence of a nested caldera. Analysis on upward continued magnetic data by recent imaging techniques highlighted two deep sources located around 5 km b.s.l., interpreted as feeding structures that are now filled with crystalline rocks. Gamma-ray data have been interpreted through integration with the geological survey results. Several previously known volcanic deposits have been identified based on radioelement distribution, and others have been redefined based on field evidence. A new succession of volcanic members is proposed, to be verified through more detailed geological mapping, geochemical analyses of rock samples and radiometric dating.

**Keywords** High-resolution airborne survey · Magnetic data · Radiometric data · Socorro Island

---

✉ V. Paoletti  
paoletti@unina.it

<sup>1</sup> Dipartimento di Scienze della Terra, dell'Ambiente e delle Risorse, University Federico II, Largo S. Marcellino, 10, 80138 Naples, Italy

<sup>2</sup> Geological Survey of Austria, Neulinggasse 38, 1080 Vienna, Austria

<sup>3</sup> Facultad de Ciencias, Universidad de Colima, Colima, Mexico

## 1 Introduction

Socorro Island (Fig. 1) is located in the eastern Pacific Ocean at  $18^{\circ}47'N$  and  $110^{\circ}58'W$ , 650 km off the coast of mainland Mexico at the intersection of the Clarion Fracture Zone and the Mathematician Ridge System, an abandoned mid-ocean ridge spreading centre. It is the most important island of the Revillagigedo Archipelago, which consists of four islands and numerous seamounts, and originates from post-abandonment alkaline magmatism (Mammerickx et al. 1988). The island has been built by both effusive and explosive volcanism during the last several hundred thousand years, fed initially by mafic magma, but more recently, large volumes have erupted with a peralkaline silicic composition (Bohrson et al. 1996), with the most recent significant subaerial activity a few thousand years ago (Farmer et al. 1993). Peralkalinity is a peculiarity of some oceanic islands, a characteristic being a molar excess of  $(Na_2O + K_2O)$  over  $Al_2O_3$ , whereas the opposite is usual in the Earth's crust (Macdonald 1974).

The last volcanic event at Socorro took place in 1993 (Siebe et al. 1995), when a submarine basaltic eruption occurred along a flank fissure that opened a few km away from the NW coast of the island. Fumarole activity (Taran et al. 2002, 2010) testifies to the current state of the island, which hosts a hydrothermal system. However, due to the remote location of the island, few studies have been carried out concerning the subsurface structure of the volcanic edifice.

Thus, a high-resolution airborne survey was conducted on the island by the *Geological Survey of Austria* in February 2009. It was the first detailed, extensive geophysical survey on the island and included magnetic, electromagnetic and gamma-ray measurements, in order to have an overall view of the main structural/lithological features. The present study only considers the magnetic and gamma-ray measurements, since electromagnetic data were measured under contract and thus are presently unavailable for research purposes.

Several active volcanic areas worldwide have been successfully investigated through the analysis and interpretation of their magnetic characteristics. Examples of relevant

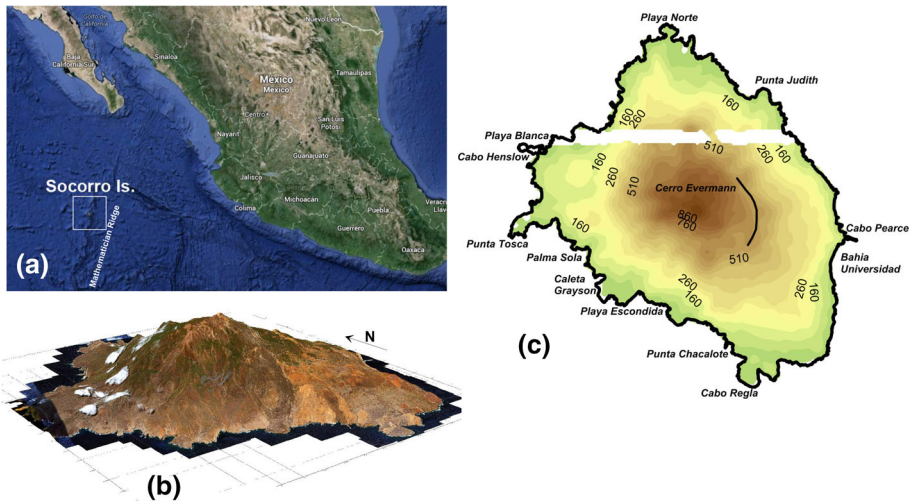


**Fig. 1** Location (a) and digital terrain model (b) of Socorro Island, Mexico. c Topography of the island based on our airborne survey. Solid line is the known caldera wall (Bryan 1966). Due to logistic problems, a limited area of the island could not be surveyed (see Sect. 3 for details)

studies of the structure of volcanoes carried out by magnetic methods are those at Piton de la Fournaise on the Réunion island, Indian Ocean (Lénat and Aubert 1982), Mt. St. Helens in Washington, U.S.A. (Finn and Williams 1987), the Canary Islands in Eastern Atlantic Ocean (Araña et al. 2000), Mount Etna (Rollin et al. 2000), the Neapolitan Volcanic Region (Paoletti et al. 2005a, b), the Aeolian Islands (Blanco-Montenegro et al. 2007) and Ustica Island (Napoli et al. 2007) in Italy. In fact, magnetic anomaly maps can provide important insights into the subsurface structure of volcanic areas because of the high magnetic response of volcanic rocks (Blanco-Montenegro et al. 2007). The interpretation of these maps can yield valuable information on the inner structure of a volcano, allowing the detection of magnetized dike-like structures possibly associated with magmatic feeding systems, and of low-magnetic materials, connected to high temperatures and/or hydrothermally altered terranes. Studies of hydrothermally altered volcanic rocks using aeromagnetic data, with implications for variable hazards, are reported in Finn et al. (2001, 2007). Furthermore, helicopter-borne acquisition allows quick measurements in rugged and inaccessible regions and can provide a satisfactory sampling of the complex magnetic anomaly pattern that often characterizes volcanic areas.

Gamma-ray spectroscopy has been used for many years for mineral exploration as well as geological and environmental mapping (e.g., IAEA 2003). Despite several borehole-, laboratory- and in situ-gamma-ray studies on volcanic rocks, not so many studies have been carried out on volcanoes using gamma-ray data from ground-based surveys (e.g., Gehring 2004; Chiozzi et al. 2009 and references therein), and even fewer have used gamma-ray airborne data (Paoletti and Pinto 2005; Aydin et al. 2006; Skácelová et al. 2009). Gamma-rays detected at airborne survey height are emitted only by approximately the uppermost 30 cm of rock (Kemski et al. 1996). Igneous rocks show a general tendency of increasing radioelement concentrations with degree of magma differentiation, as clearly shown by mildly alkaline and peralkaline volcanics (e.g., Bohrson and Reid 1995; Civetta et al. 1998). Furthermore, felsic volcanic rocks often show very high radioelement concentrations compared to average crustal abundances. Thus, gamma-ray spectroscopy could be an appropriate technique for studying and deriving knowledge on the magmatic evolution and the different eruption phases of a volcano.

The application of these techniques is particularly suitable for the island of Socorro given its remote location and difficult accessibility of large areas due to the intense vegetation. Thus, the aim of this work is to retrieve information about the surface and subsurface geology of Socorro Island based on the analysis and interpretation of magnetic and gamma-ray airborne data, integrated with available geological information from the literature and enhanced through a new field survey. The island is still active as testified by the most recent eruption which occurred about 20 years ago, as well as the occurrence of fumarole emissions near its summit. Volcanic hazard is high due to the explosive character of its past activity on the one hand, and the peculiarity of peralkaline lava flows, that are particularly fast flowing, on the other hand. Hence, this study is of particular relevance for the evaluation of volcanic risk on Socorro.

## 2 Geological Outline

### 2.1 Geography and Topography

With an extent of about 130 km<sup>2</sup>, Socorro is the largest island of the Revillagigedo Archipelago, which includes also the islands of Clarión, San Benedicto and Roca Partida,

each one being volcanic in origin. These four islands as well as a group of several seamounts make up the Mathematician Ridge (Fig. 1a), an abandoned mid-ocean spreading centre which was active from 6.5 to 3.15 Ma before present (Mammerickx et al. 1988).

Socorro Island (Fig. 1b, c) is the emergent portion of a large shield volcano, which rises from the seafloor at a depth of about 3 km to the summit of the volcano at 1050 m above sea level, and has a submarine slope of a little more than 10 degrees (Bryan 1966). With a basal radius of 24 km and the assumption that the volcano is a perfect cone, the total volume of the volcano is approximately 2400 km<sup>3</sup>. The subaerial portion of Socorro represents only about 2 vol% of the total edifice.

It has been proposed that a topographic feature, i.e. a steep escarpment a few metres high found at approximately 600-m elevation on the south-eastern side of the summit (Fig. 1c), is the only remnant of a collapse caldera wall (Bryan 1966). The curvature and size of the steep escarpment are consistent with a former caldera dimension of about 4.5 by 3.8 km, which is typical for peralkaline volcanoes (Bohrson et al. 1996). Such a caldera collapse would have been related to some large explosive eruption and concurrent emplacement of an ignimbrite, as described later.

## 2.2 Composition of the Rocks and Volcanic History

Volcanism in the Revillagigedo Archipelago has produced a bimodal association of mafic (mostly alkali olivine basalts, hawaiites and mugearites) and silicic (soda-rich, peralkaline trachytes and rhyolites) rocks, resulting from both explosive and effusive eruptions (Bryan 1966; Moore 1970; Baker 1974; Farmer et al. 1993; Carballido-Sanchez 1994; Bohrson and Reid 1995; Davis et al. 1995; Bohrson et al. 1996). Socorro Island's eruptive history was characterized by an early shield-building stage, with basaltic effusive eruptions, and late extensive pyroclastic eruptions fed by peralkaline silicic magmas which produced small volumes of products, though they dominate the surface of the island. The dominant subaerial peralkaline silicic products, and especially the occurrence of pantellerites (i.e. peralkaline rhyolites), make Socorro Island virtually unique in the Pacific Ocean, and similar to the island of Pantelleria located in the Sicily Channel Rift Zone, Southern Italy (e.g., Civetta et al. 1998). Similarly to Pantelleria, silicic rocks from Socorro Island have a peralkalinity index, also known as agpaitic index, i.e. molar  $(\text{Na}_2\text{O} + \text{K}_2\text{O})/\text{Al}_2\text{O}_3$ , of 1.1–2.2 (Bohrson and Reid 1997). According to Carballido-Sanchez (1994), almost 90 % of the peralkaline products exposed on Socorro Island are of pantelleritic composition. There is no evidence to indicate variations in magma composition during the prolonged construction of the shield edifice. Thus, assuming that the submarine portion of the volcano is composed mainly of basalts, peralkaline silicic rocks make up only 1.5 vol% of the volcanic edifice. However, in reality, only little is known about the submarine part of the volcano.

The oldest subaerially exposed deposits of Socorro Island are 540-ka-old alkaline basalts to comendites, which are confined to the base of a sea cliff at the eastern part of the island (Bohrson et al. 1996; Bohrson and Reid 1998). Given the topographic and geological evidence for a caldera collapse, the eruptive history of the emerged portion of the island has been divided into pre-, syn- and post-caldera stages (Bryan 1966; Bohrson et al. 1996). After the volcano broke the surface of the Pacific Ocean, activity transitioned to more explosive with the deposition of mostly peralkaline silicic pyroclastics, with a total thickness of about 150 m, dated radiometrically at between 540 and 370 ka (Bohrson et al. 1996). These were described by the authors as commonly holocrystalline, non-vesicular lava-like deposits and defined as ignimbrites. However, in a later work Sbarbori et al.

(2009) report an absence of welding within the same deposits and classified them as lava flows interbedded with surge and ash deposits. No morphological evidence was found for an early caldera collapse related to the pre-caldera pyroclastics.

It has proved a challenge to separate unequivocally the deposit formed during the landmark caldera-forming eruption. Caldera formation occurred probably around 370 ka and was followed by up to 200 ka of quiescence. It was an important event, the only major explosion that has recorded a clear morphological feature, and it seems it marked a fundamental change in the eruptive characteristics of the volcano. Afterwards, a change in eruptive style from predominantly explosive to predominantly effusive occurred (Bohrson et al. 1996). Rocks of the post-caldera stage have been subdivided, based upon composition, into: the Cerro Evermann deposits (emplaced between 182 and 15 ka) and Lomas Coloradas deposits (between 150 and 5 ka) (Farmer et al. 1993; Bohrson et al. 1996). Rocks of the Cerro Evermann deposits are pyroclastics, lava flows and lava domes of peralkaline composition, exposed in the caldera and at the northern, western and southern flanks of the volcano. These are primarily trachytes, comendites and pantellerites. The lava flows and cinder cones of the Lomas Coloradas deposits are exposed at the south-eastern part of the island and are composed of basalt, hawaiite and mugearite (Carballido-Sanchez 1994). Eruption of peralkaline-rhyolitic and basaltic magmas during the same time interval of post-caldera phase has been explained by a stratified magma chamber composed of soda-rhyolite overlying basaltic magma (Bryan 1966).

Morphologically, the subaerially exposed rocks on Socorro Island can be classified as lava flows, domes, pyroclastic flows, air-fall pyroclastics and cinder cones. The lava flows on Socorro Island are of both basaltic and peralkaline silicic composition, whereas the pyroclastic flow deposits are exclusively peralkaline silicic. Cinder cones are generally basaltic in composition (except for one) and are confined to the Lomas Coloradas deposits, with an additional occurrence at Playa Norte. The domes, on the other hand, are exclusively peralkaline silicic, being of much higher viscosity. Tephra of both silicic and basaltic composition can be found at many locations across the island (Carballido-Sanchez 1994).

The presence of a small summit caldera on Socorro suggests that the silicic magma reservoir was shallow, probably located within the volcanic edifice or the upper oceanic crust. Previous studies on peralkaline volcanoes found evidence for depths of a few kilometres for the magma chambers feeding silicic eruptions (Mahood 1984; Mahood and Baker 1986). Recent melt inclusions and experimental petrology investigations (Di Carlo et al. 2010; Gioncada and Landi 2010; Lanzo et al. 2013) on peralkaline trachytes and rhyolites have constrained the depth of magma reservoirs at Pantelleria island. A depth of 2–3 km has been estimated for the reservoir that fed the large, caldera-forming Green Tuff eruption (50 ka BP), whereas 4–5 km is the estimated depth for the reservoirs that fed younger (<20 ka BP), small-volume, both effusive and mildly explosive eruptions. Given the analogy between Pantelleria and Socorro islands, it is likely that similar depths might have characterized the magma reservoirs of the latter.

Volcanic activity on Socorro Island has continued to the present. The first historically reported eruption took place in 1848, then another was observed in 1896, but no detailed description of the two exists. A further small eruption was reported in 1951 (Bryan 1966), possibly phreatic, though no field evidence exists. The most recent eruption occurred in 1993 2.4 km NW of Punta Tosca, producing floating scoria and reticulite of hawaiitic composition (Siebe et al. 1995). Currently, extensive fumarole activity can be observed near the summit associated with a well-developed hydrothermal system. The geochemistry of hydrothermal fluids discharged on the island has been investigated by Taran et al. (2010).

### 2.3 Evidences from the New Geological Survey

During this study, an analysis of previous mapping (Bryan 1966; Carballido-Sanchez 1994; Bohrson and Reid 1997) enhanced by fieldwork has resulted in a new geologic sketch map of Socorro (Fig. 2).

Changes in topography were analysed with a detailed revision of satellite images and aerial photographs (Fig. 3). This allowed us to adjust some of the boundaries between

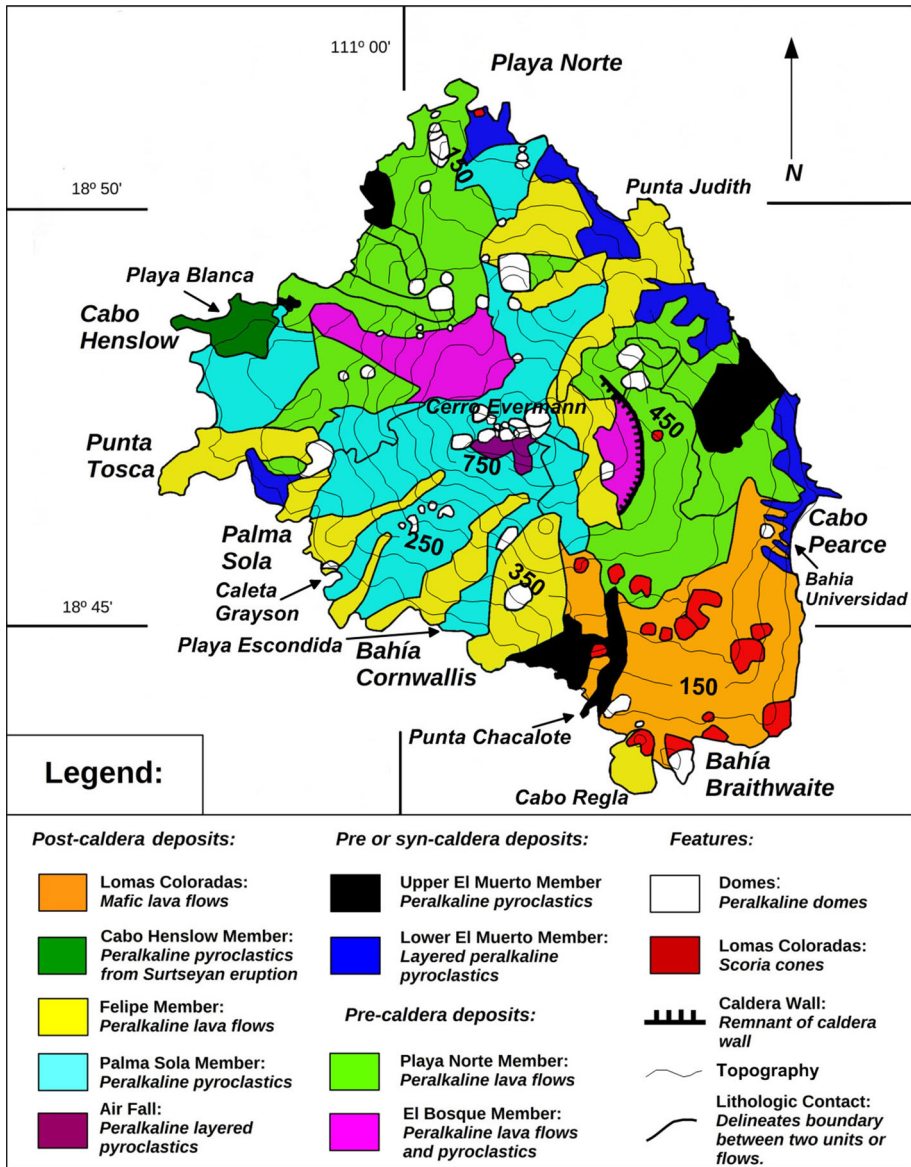


**Fig. 2** New geologic sketch map of Socorro Island based on previous studies (e.g., Carballido-Sanchez 1994) and a new geologic survey (this work)



deposits as well as reclassify others based on textures of the terrain, features such as pressure ridges and levees of lava flows, or vegetation and colouration. Effusive features, namely domes and lava flows, have been delimited in the new map. The origin of many deposits has been debated in the few previous studies, in some cases whether they are the products of effusive or explosive volcanism. Such fundamental questions have clear implications for the assessment of future hazards scenarios on the island.

Leaving boundary adjustments aside, some of the more significant changes in map are summarized below:

1. Previously the pre- or syn-caldera deposits had been divided between the Playa Blanca and El Muerto members (Carballido-Sanchez 1994). The deposits closest to the Playa Blanca location are now thought to be associated with a Surtseyan eruption consisting of a large series of surge deposits. This has been named the Cabo Henslow Member, whereby the previous Playa Blanca pyroclastic member has been renamed to the Upper El Muerto Member.
2. Several areas previously identified as being covered by pyroclastics have now been included in the Playa Norte lava flow Member.
3. The Palma Sola post-caldera pyroclastic Member now covers the area close to Bahía Cornwallis, previously included in the Lomas Coloradas (Carballido-Sanchez 1994). Some areas previously identified as pre-caldera have also been reclassified as part of the Palma Sola Member.



**Fig. 3** Punta Tosca—prominent peralkaline lava flow showing levees and pressure ridges. To the right, a group of small domes can be seen

- Further post-caldera peralkaline lava flows have been attributed to the Felipe Member, previously grouped into the poorly defined El Bosque pre-caldera flow and pyroclastic member and another part of the previous Playa Blanca member.

### 3 Survey Layouts and Data Processing

In 1999, a geophysical survey was carried out in the south-eastern part of Socorro Island with the use of five portable broadband seismometers (Valenzuela et al. 2005). The intention was to install a seismic T-phase station on Socorro, as part of the International Monitoring System (IMS) of the Comprehensive Nuclear-Test-Ban Treaty Organization (CTBTO). The airborne geophysical and ground geoelectric survey of the *Geological Survey of Austria* (GSA) in 2009 was the first detailed extensive geophysical survey on Socorro Island (Fig. 4a). Previous surveys had been largely limited to the hydrothermal area near to the summit (e.g., TEM, magnetic surveys, self-potential and CO<sub>2</sub> flux; Varley et al. 2004). The remote location of the island necessitated extensive logistic preparations, which were successfully undertaken by the Mexican navy. A MI17-type helicopter was

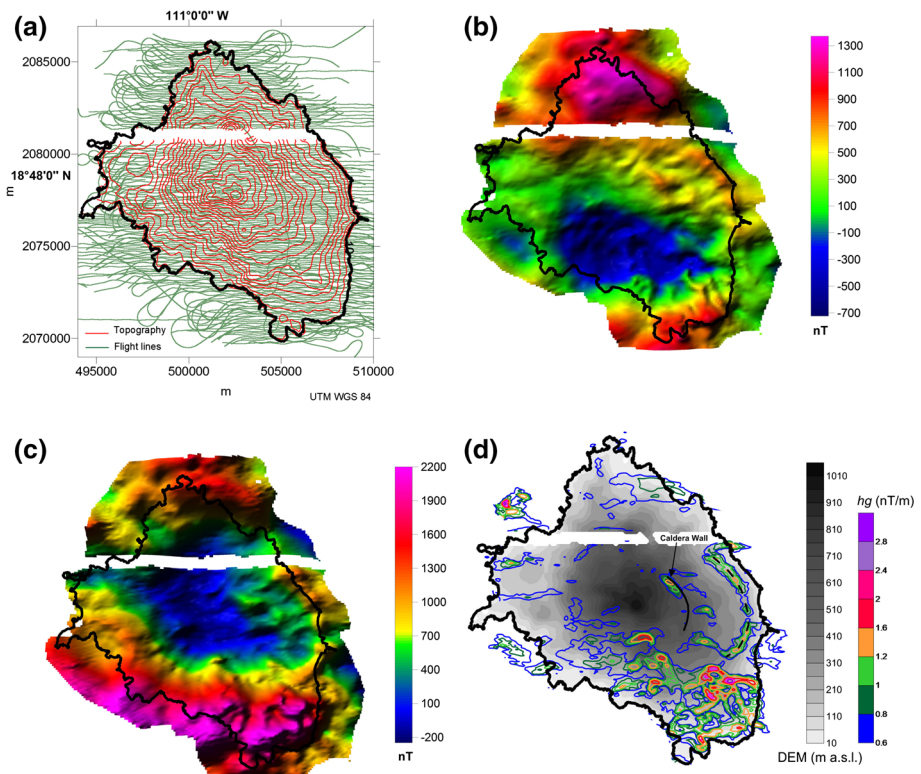


**Fig. 4** **a** Helicopter-borne lines flown over Socorro during the 2009 survey, with an average spacing of 100 m; **b** draped magnetic map (clearance about 100 m); **c** pole-reduced data; **d** maxima of the horizontal gradient data ( $hg$ ) (colour contours) overlapped to the topography of the island (grey scale). Solid line is the known caldera wall (Bryan 1966), and dashed line is the caldera rim inferred in this study



provided by the Mexican marines for transport of the crew and equipment from Manzanillo (Mexico) to Socorro and to perform the survey. To acquire high-resolution electromagnetic, magnetometric and gamma-ray data we used the complex airborne system of the *Geological Survey of Austria* (Motschka 2001; Paoletti et al. 2005a, b). Its instrumentation consists of a frequency domain electromagnetic sensor operating at four different frequencies, a magnetic sensor (a caesium magnetometer having a sensitivity of 0.01 nT) and a gamma spectrometer equipped with NaI crystals.

The survey, carried out in February 2009, covered an area of 200 square kilometres, with E-W flight lines and an average line spacing of 100 m. The use of an electromagnetic system (along with magnetometric and gamma-ray instrumentation) required the distance between terrain and sensor (“bird”, dragged 30 m below the helicopter) to be constantly less than 100 m, in order to yield a reliable subsurface resistivity mapping. However, during the field measurements, it turned out that these requirements about spacing and clearance could not be fulfilled for all parts of the surveyed area. Due to the rough terrain of the island, a sensor clearance of 100 m was very difficult to be constantly maintained without endangering the safety of the helicopter and crew. Furthermore, during the ongoing survey, it turned out that a part of the fuel supply, already deposited on the island before the survey, was contaminated. Due to the remote distance of the island, additional barrels could not be obtained in due time. Thus, six lines in the middle part of the island were not surveyed and the western offshore of the island could not be covered. The spacious turning loops over the sea area were necessary since calibration of the system had to be performed at high altitudes above 400 m after at least each second line. Positioning was performed using the data of a laser altimeter, two differential GPS sensors and flight path recordings from a downward-looking digital video camera. For correction of altitude raw values for variations in vegetation thickness, we employed advanced algorithms.

The processing of the magnetic data measured over Socorro included the following steps: (1) removal of spikes and gaps in the data; (2) flight path check and repositioning, which consisted of the removal of wrong coordinates, correction of the GPS data, and a revision of the flight altitude; (3) Earth’s magnetic field diurnal variation correction, which was performed using the data from a base station located on the island; (4) removal of the International Geomagnetic Reference Field (IGRF).

Natural gamma radiation is essentially derived from the radioactive elements potassium ( $^{40}\text{K}$ , energy peak: 1.46 MeV), uranium ( $^{238}\text{U}$ , energy peak: 1.76 MeV) and thorium ( $^{232}\text{Th}$ , energy peak: 2.62 MeV). Gamma-ray spectrometers which are used for airborne surveys usually consist of up to eight large, thallium-activated sodium iodide NaI(Tl) crystals which are connected to a 256-channel spectrometer. Prior to processing, data were inspected for incorrect values and all samples taken at an altitude higher than 250 m were deleted.

Processing was performed with the use of PCA (Principal Component Analysis) smoothed spectra (Hoovgard and Grasty 1997); radon signal removal was performed using the spectral-ratio method. In some parts of the island (especially in the south-western part), the height correction did not work well due to large differences in flight altitude of the helicopter between adjacent flight lines. This resulted in lower ground concentrations for high flight altitudes and higher ground concentrations for low flight altitudes for a few areas of the island.

## 4 Magnetic and Gamma-Ray Data

In Fig. 4b, we show the draped aeromagnetic map of Socorro obtained after the mentioned processing procedure (Sect. 3) and data gridding by the *kriging* interpolation method, with a grid-node spacing of 100 m and search radius of 150 m. The field is characterized by a dipolar anomaly of about 2000 nT amplitude whose maximum–minimum orientation is non-aligned with the direction of the present Earth’s magnetic field (inclination  $44^\circ$  and declination  $9^\circ$ ). These characteristics may be related to the presence of sources with a component of remanent magnetization or to other causes, as discussed below.

In order to locate the position of the magnetic sources of the anomalies of the island, we computed pole-reduced data by accounting for the presence of sources with a component of remanent magnetization. Characteristic values were taken from the studies carried out by Sbarbori et al. (2009), who found values of  $40^\circ$  and  $357^\circ$  for the remanent inclination and declination, respectively. In Fig. 4c, we show the so-obtained pole-reduced map referred to a draped acquisition surface with a clearance from the topography of about 100 m.

Figure 5a–c shows the measured gamma-ray data for the three radioelements ( $^{40}\text{K}$ ,  $^{238}\text{U}$  and  $^{232}\text{Th}$ ), whereas in Fig. 5d we show a ternary radioelement map of the island, obtained by assigning the colours red, green and blue to the channels of potassium, thorium and uranium, respectively. Combinations of the radioelement concentrations are displayed as combinations of the three mentioned colours, whereas black and white represent, respectively, very low and very high concentrations of all three radioelements. If mainly two radioelements are present, same amounts of K and Th are displayed as yellow, while same amounts of K and U are displayed as magenta and same amounts of Th and U are displayed as cyan.

The best gridding results for the gamma-ray data could be achieved with the gridding method *kriging* and using the same parameters as for magnetic data.

## 5 Interpretation

### 5.1 Magnetic Data

The draped pole-reduced map (Fig. 4c) shows a large negative anomaly located in the central part of the island, corresponding to the summit of Socorro, and extending south-eastward. This may be connected to: a high-temperature zone (above the Curie temperature) in the deeper part of the volcano due to a magma body, and/or a low total remanent magnetization of pyroclastic caldera sediments due to non-aligned sedimentation, and/or the influence of hydrothermal alteration within the caldera. Geochemical studies on the geothermal system of the island (Taran et al. 2010) identified temperatures of  $500\text{--}600^\circ\text{C}$  by using chemical and isotopic geothermometers, while a TEM survey revealed a perched water body beneath zones of extensive hydrothermal alteration (Varley et al. 2004). This outcome seems to favour the first hypothesis.

To locate the lateral boundaries limiting the magnetic sources of the island, we used the location of maxima of the horizontal gradient ( $hg$ ) of the pole-reduced draped magnetic field (Grauch and Cordell 1987; Grauch et al. 2001; Pilkington and Keating 2004; Verdusco et al. 2004; Nabighian et al. 2005; Cooper and Cowan 2006). The  $hg$  data superimposed on the topography of the island (Fig. 4d) show a rather good match between the

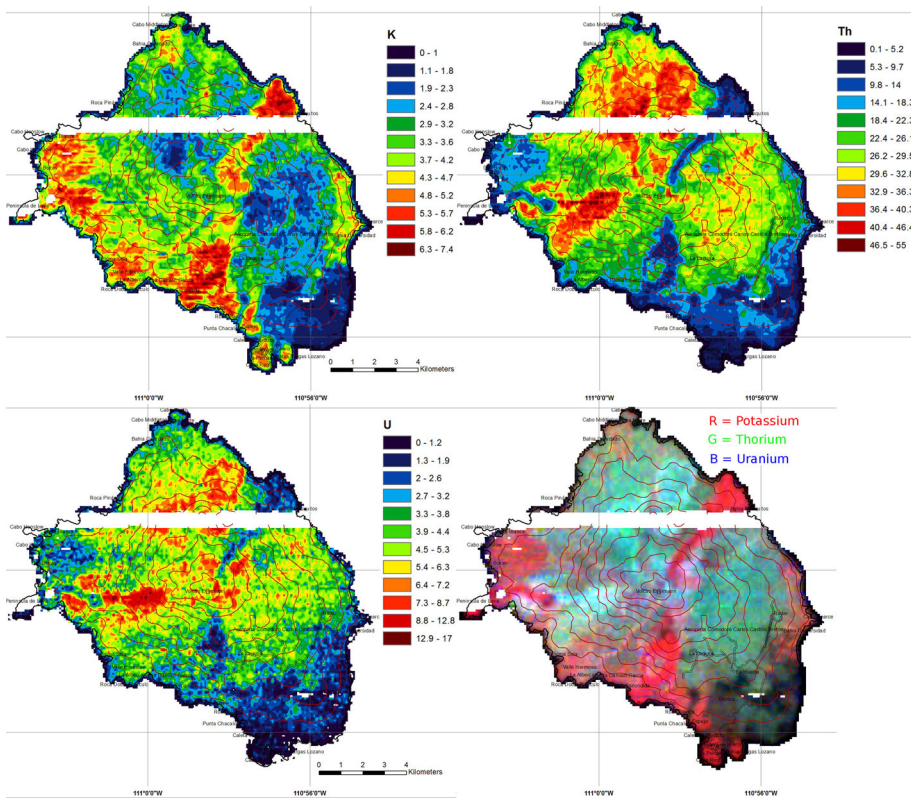


**Fig. 5** Gamma-ray data at Socorro: **a** potassium radioelement map (%); **b** uranium radioelement map (ppm); **c** thorium radioelement map (ppm); **d** ternary radioelement map of Socorro Island. Maps were obtained through NASVD smoothing (Hoovgard and Grasty 1997)

maxima of the  $hg$  data and the known position of structures. More specifically, the curved maxima of the  $hg$  data in the central sector of the island are located just above the caldera wall (dated around 370 ka), as inferred by Bryan (1966). We also note a complex pattern of maxima in the southern area of the island, corresponding to the northern edge of the Lomas Coloradas Member.

A striking feature of the map is the presence of another trend of curved maxima located east of the known caldera wall. This may be related to some terrain effect, which can be significant over rugged topographies (Grauch and Cordell 1987). Nevertheless, an examination of possible correlations between topography and horizontal gradient maxima showed that the  $hg$  maxima are located over some topographic ridges only in some cases, whereas the curved pattern of the  $hg$  maxima is rather continuous also over non-rugged areas. This suggests the possibility that the caldera has a nested structure, i.e. an older collapse event might have occurred affecting a larger area of the island. The oldest pyroclastic deposit on Socorro (ignimbrites according to Bohrsen et al. 1996, lavas and pyroclastics according to Sbarbori et al. 2009) might be related to such an event. Even though nested calderas have been reported for a number of peralkaline edifices such as Pantelleria (Mahood and Hildreth 1983; Mahood 1984),

Bohrson et al. (1996) note that structural evidence for nested calderas is absent or buried at Socorro.

In order to study deep-seated magnetic structures and their possible connection with the inverted pole-reduced anomaly in the central section of the island, we continued the data upward to a constant altitude of 1200 m a.s.l. and computed the total gradient ( $tg$ ) of the data (Fig. 6, upper plot). Data were continued from an uneven surface to a flat one through an algorithm based on an equivalent source procedure, with the draped acquisition surface being approximated by a polyhedral surface (Ivan 1994). Given the relatively small extent of the survey area, in order to adequately represent low frequencies, we performed the continuation on a larger dataset built through extrapolation algorithms (e.g., Mastellone et al. 2014) and extending outside the survey area.

It is known (e.g., Roest et al. 1992) that the maxima of the  $tg$  are located directly over the sources, independently from the possible presence of remanence. The  $tg$  map of upward continued data (Fig. 6, upper plot) at Socorro is characterized by maxima both in the northern and southern sectors of the island in correspondence mainly with the post-caldera eruptives, highlighting the presence of deep and wide sources. An estimation of the depth of those structures was yielded by the use of the *Depth from Extreme Points method (DEXP)* (Fedi 2007; Fedi and Pilkington 2012), a multi-scale imaging technique. This method allows assessing the source's depth and *structural index* (a parameter related to the source type, e.g., Paoletti et al. 2013) from the extreme points of a 3D field, scaled according to specific power laws of the altitude. The source location and depth are imaged as maxima of the *DEXP* signal, whereas the *structural index* is related to the scaling exponent of the power laws of the altitude. Even though the *DEXP* method may yield estimates on the source dipole moment as well, for Socorro we were able to obtain a qualitative estimation of the sources magnetization  $M$  in relative terms. The outcome (Fig. 6, lower map) shows two large sources, a deeper one located to the north (depth

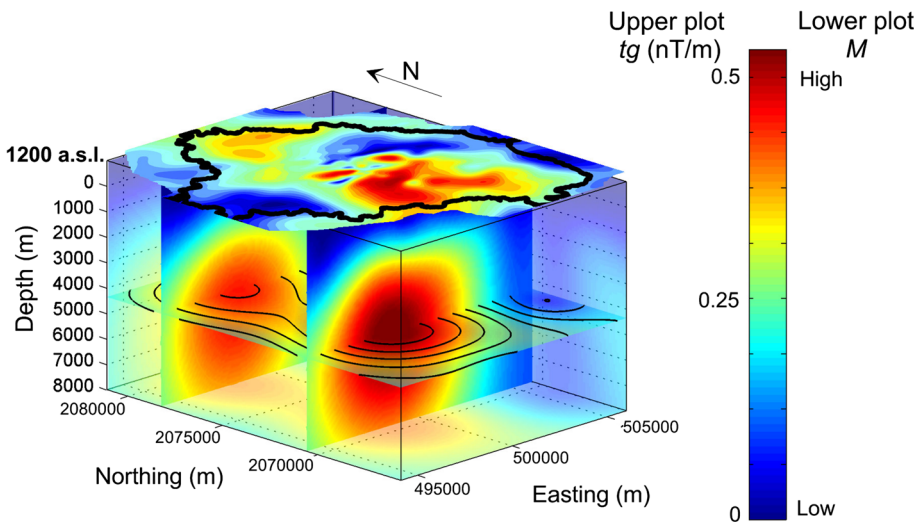


**Fig. 6** Imaging of Socorro's deep magnetic structures through the *DEXP* method (Fedi 2007). The *upper map* shows the data used for the analysis, i.e. the total gradient  $tg$  of the upward continued data. The *lower plot* is the result of the *DEXP* analysis and highlights two large magnetized sources located between 4.5 and 5 km b.s.l. Note the same colour scale for the two datasets ( $tg$  and *DEXP*)

5 km b.s.l.) and a larger and slightly shallower one located to the south (depth 4.5 km b.s.l.). An estimation of the *structural index* for the two sources yielded a value of about 2, which is consistent with vertical cylinder-shaped sources. Thus, we tentatively interpret those sources as feeding structures that are now filled with crystalline rocks. These structures may represent the peripheral colder portions of a central volume whose temperature is still above the Curie point. We note that the results refer to the deep-seated structures, rather than to shallower-local structures, because of the low-pass filtering effect of upward continuation which attenuates the shallow-sourced responses. The inferred depths refer to the top of the sources (Cella and Fedi 2012) and are in agreement with the results from studies on peralkaline edifices (see Sect. 2, e.g., Mahood and Baker 1986; Lanzo et al. 2013). Moreover, a heat source located 4–5 km below the island is consistent with the occurrence of a shallow hydrothermal circulation and hot gaseous emissions at surface (Taran et al. 2002, 2010).

## 5.2 Gamma-Ray and Geological Data

Interpretation of gamma-ray data was carried out in the light of the results of our new geological survey. Table 1 shows an overview of the main lithological members and their chronology, whereas in the following subsections we give a description of the correlation between gamma-ray data and the deposits. The members highlighted by our radiometric data interpretation are shown in Fig. 7.

### 5.2.1 Pre- and Syn-caldera Deposits

**5.2.1.1 Lower El Muerto Member** The Lower El Muerto Member in the Cabo Pearce area represents the oldest crystalline tuff and is probably the oldest exposed pre-caldera peralkaline pyroclastic flow deposit. Deposits can be found along the eastern shoreline of

**Table 1** Chronology of volcanic products on Socorro Island (eruption periods after Carballido-Sanchez 1994; Bohrson et al. 1996; Farmer et al. 1993); capital letters next to the members refer to the deposit's designation from Bohrson et al. (1996)

Period of deposits	Composition/age	Members	K	U	Th
Post-caldera	Silicic peralkaline/trachyte deposits 182–15 ka	Felipe Member	4.5	4.4	9.4
		Palma Sola Member	3.6	6.2	23.0
		Grayson Member	3.8	8.1	31.6
		Domes 1	3.7	6.9	25.9
		Domes 2	4.3	2.1	6.7
		Cabo Regla Flow	4.2	2.2	6.5
	Lomas Coloradas basaltic deposits <150–5 ka	Lomas Coloradas	2.0	3.6	13.2
		Scoria Cones	1.6	3.1	10.0
		Cabo Regla Scoria Cone	4.0	2.2	8.1
Pre-syn-caldera	~ 384–367 ka	El Bosque Member	2.1	7.2	29.8
	unknown	Playa Norte Member ( <b>E</b> )	2.6	7.1	29.0
	~ 433–420 ka	Upper El Muerto Member ( <b>D</b> )	4.4	4.3	14.8
	~ 480 ka	Lower El Muerto Member ( <b>C</b> )	3.7	4.7	17.8

The last three columns show average radioelement concentrations for each member: K [%], U [ppm], Th [ppm]



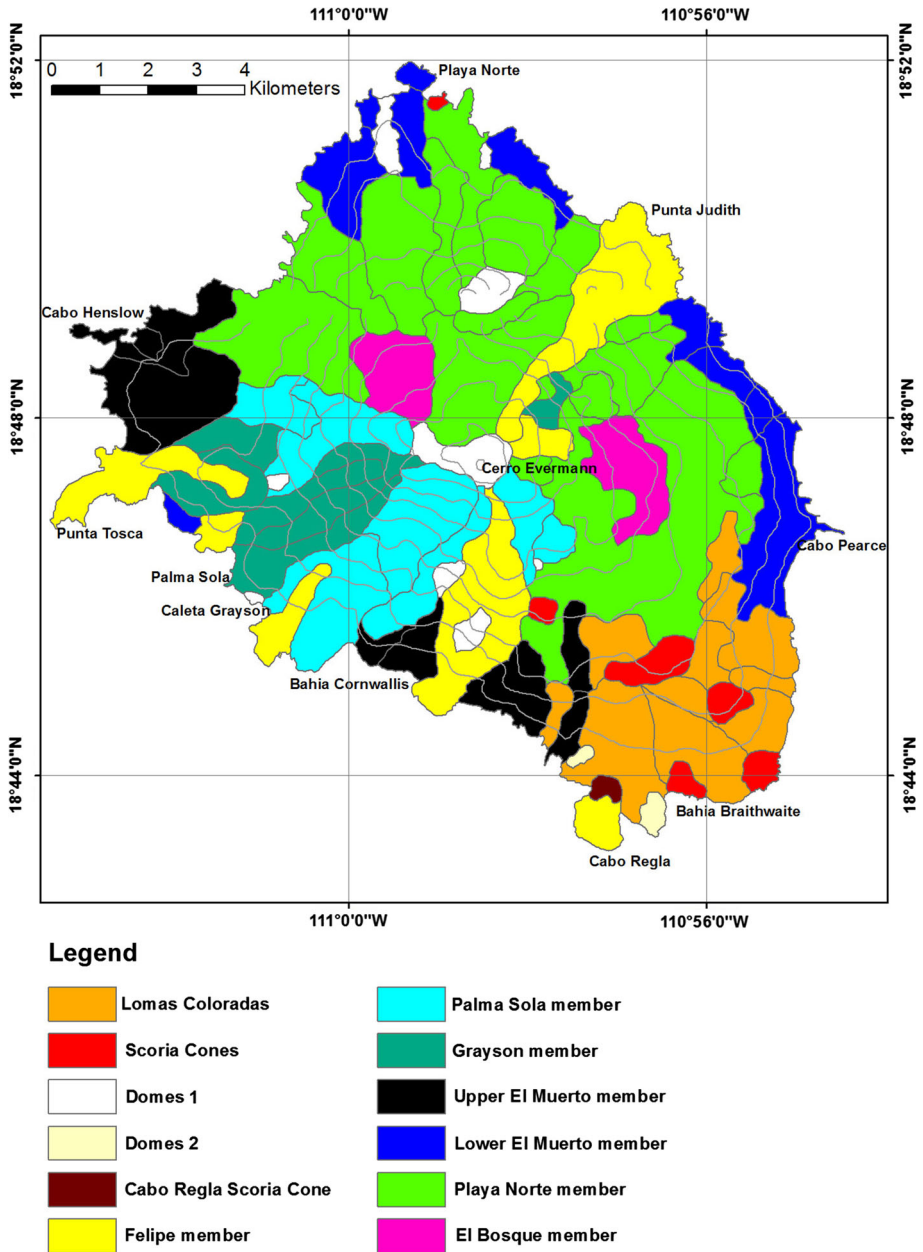


**Fig. 7** Map of the different geological members considering the radiometric data

the island, partly capped by younger pyroclastic products (Carballido-Sanchez 1994). The earliest exposed basaltic deposits are found beneath these layers (Bryan 1966).

Further deposits of the Lower El Muerto Member have been identified south of Punta Tosca and along the northern coast, but the latter could not be clearly identified by

radiometric signatures of the present study. The deposits of the Lower El Muerto Member show average radioelement concentrations of 3.7 % K, 4.7 ppm U and 17.8 ppm Th.

**5.2.1.2 Upper El Muerto Member** The peralkaline pyroclastic flow deposits of the Upper El Muerto Member are crystalline tuffs, which are slightly younger than the tuffs of the Lower El Muerto Member. Carballido-Sanchez (1994) classified them as pantelleritic trachytes and found several deposits across the island. On the basis of radiometric results, only some deposits along the south-western coastline could be clearly identified. One deposit, which is located in the Cabo Henslow area, has been mapped as Cabo Henslow and Palma Sola members; however, its radiometric signature suggests it belongs to the Upper El Muerto Member. Three other deposits, which are mapped in the eastern and north-western part of the island as belonging to the Upper El Muerto Member, show different radiometric properties and so are interpreted as having a different origin. The mean radioelement concentrations of this member are 4.4 % K, 4.3 ppm U and 14.8 ppm Th.

**5.2.1.3 Playa Norte Member** The Playa Norte Member consists of peralkaline lava flows which were sampled by Carballido-Sanchez (1994) in the eastern and north-western sector of the island. Further flows were defined by the interpretation of aerial photographs and have been defined as either pre- or syn-caldera. The terranes belonging to the Playa Norte Member recognized in the present work (Fig. 2) could not be clearly identified by their radioelement signature alone. Their possible distribution was determined by comparing the radioelement maps with the satellite image and the geological map. Deposits were found in the north-western sector of the island and showed mean radioelement concentrations of 2.6 % K, 7.1 ppm U and 29.0 ppm Th. It is noteworthy that this member shows a particularly low K content, but very high U and Th contents.

**5.2.1.4 El Bosque Member** Crystalline peralkaline pyroclastics of the El Bosque Member are younger than the Upper El Muerto Member. Limited exposures found by Carballido-Sanchez (1994) make up large parts of the caldera wall, and therefore this member could possibly be associated with its formation. Due to dense vegetation and difficult access, only the outcrops east of the caldera were sampled by that author and their distribution defined by means of morphological similarities in aerial photographs. The only outcrops identified in this study, which coincide with El Bosque outcrops defined by Carballido-Sanchez are those found east of the caldera and to the northwest of Cerro Evermann. The two areas representing the El Bosque Member differ from the surrounding Playa Norte Member by their lower potassium concentration, 2.1 % on average, whereas U and Th are similarly high, 7.2 and 29.8 ppm, respectively.

## 5.2.2 Post-caldera Silicic Flows

**5.2.2.1 Felipe Member** Carballido-Sanchez (1994) recognized at least ten peralkaline lava flows, which he assigned to the Felipe Member. These included the evidently visible lava flows of Punta Tosca, Punta Judith, Bahia Cornwallis, Caleta Grayson and those close to the summit area. Investigation of the present dataset only allowed a delineation of the lava flows that form Punta Tosca, Punta Judith, a flow to the south of Palma Sola and the lava flow that reaches the coast at Playa Escondida, as they are clearly identified as negative thorium and positive potassium anomalies. Surprisingly, the above-mentioned

author assigned the latter flow to the Lomas Coloradas Member. Bohrsen et al. (1996) also determined this flow to be composed of peralkaline trachyte and dated it at approximately 15 ka; it clearly can be assigned to the Felipe Member. These four peralkaline lava flows have very similar radioelement concentrations of about 4.5 % K, 4.4 ppm U and 9.4 ppm Th.

Furthermore, Fig. 2 shows seven other peralkaline lava flows characterized as Felipe Member; however, their radioelement signature is different. While their potassium concentration is close to that of the other terranes attributed to the Felipe Member (~4.5 % K), they show distinctly higher concentrations in uranium and thorium (5.8 ppm U and 18.7 ppm Th).

**5.2.2.2 Palma Sola Member** The Palma Sola is the most recent member made up of peralkaline crystalline pyroclastics and forms part of Bryan's (1966) Cerro Evermann eruptives. It is the only crystalline pyroclastic member, which can be considered unequivocally post-caldera in age (Carballido-Sanchez 1994).

In this study, important differences have been noted between the mapped terranes attributed to the Palma Sola Member and their radiometric signature. The area to the west of the island appears in the potassium map as a high K anomaly. In the thorium map, a large positive Th anomaly appears within this area, which is absent in the other areas recognized as belonging to the Palma Sola Member. To distinguish between those two areas, the high Th zones have been designated as the Grayson Member, a new deposit defined in this study (see Table 1). With an average of 31.6 ppm Th, the Grayson Member shows the highest thorium concentrations of all members, and high concentrations of potassium (3.8 %) and uranium (8.1 ppm). The Palma Sola Member shows lower mean radioelement concentrations (especially thorium) of 3.6 % K, 6.2 ppm U and 23.0 ppm Th.

**5.2.2.3 Domes 1** Domes on Socorro Island are either comenditic or pantelleritic in composition. In general, domes are typical for late stages of volcanic activity when the final ascending magma is more degassed, crystal-rich and hence more viscous. Bryan (1966) found similarities between the comenditic domes on Socorro Island concerning their composition, structure and degree of weathering, and hence concluded that most had formed during the latest stage of activity.

At least thirty domes (or groups of domes) have been identified on Isla Socorro. The gamma-ray signatures of the larger ones were identified. Differences with the surrounding members are not always very clear, either because some of them are too small to appear as anomalies in the radioelement maps or because the surrounding deposits have similar radioelement concentrations. Mean radioelement concentrations of the peralkaline domes are 3.7 % K, 6.9 ppm U and 25.9 ppm Th.

**5.2.2.4 Domes 2** A separate dome definition is proposed and refers to two peralkaline trachyte domes in the southern part of the island, since they have a different radiometric signature as compared to the other Socorro domes having lower Th values. These represent some of the most recent extrusions of silicic magma on the island and postdate the Lomas Coloradas mafic flows. In the studies of Bohrsen et al. (1996), their  $^{40}\text{Ar}/^{39}\text{Ar}$  ages were determined to lie between 60 and 70 ka.

They show high potassium concentrations averaging 4.3 %, and low uranium and thorium concentrations averaging 2.1 and 6.7 ppm, respectively. They might belong to another eruptive cycle.

### 5.3 Lomas Coloradas Area

The Lomas Coloradas area is the most accessible part of Socorro and covers approximately 20 % of its surface area. It is the youngest major deposit of the island and consists of lava flows and scoria cones of basaltic, mugearitic and hawaiitic composition (Carballido-Sanchez 1994; Bohrson et al. 1996). Most of the previous geological and geochemical studies on Socorro Island have been confined to this area, and therefore considerably more information is available. Here, the lowest concentrations of all three radioelements on the entire island have been clearly identified by gamma-ray spectrometry.

#### 5.3.1 Lomas Coloradas Basalt Lava Flows

Although Socorro Island is believed to be composed mainly of basalts, the Lomas Coloradas alkaline basalts, which are confined to the south-eastern part of the island, are the only ones exposed at the surface. The basalts have erupted from fissures on the flanks or from the base of cinder cones, and show typical pahoehoe morphology with the formation of lava tubes.

Contacts between basalts and pre- and syn-caldera deposits show that the basalts are younger, whereas contacts between Lomas Coloradas basalts and domes demonstrate that these two deposits were emplaced by contemporaneous eruptions (Bohrson et al. 1996). As expected on the basis of their mafic composition, the Lomas Coloradas basalt lava flows are characterized by low concentrations of 2.0 % K, 3.6 ppm U and 13.2 ppm Th.

#### 5.3.2 Scoria Cones

Scoria cones show the lowermost radioelement concentrations of the island. At least ten deposits could be identified by their gamma-ray signatures. According to Carballido-Sanchez (1994), more than 18 scoria cones can be found in the Lomas Coloradas area. One anomalous cone is found close to Playa Norte. The scoria cones have mean radioelement concentrations of 1.6 % K, 3.1 ppm U and 10.0 ppm Th; particularly, the thorium concentrations are significantly lower than those of the surrounding Lomas Coloradas basalt lava flows.

The scoria cone at the top of the lava flow forming Cabo Regla represents an exception within the other scoria cones and has therefore been assigned to an own member (Cabo Regla Scoria Cone). It shows similar radioelement concentrations as the lava flow at Cabo Regla, which has been interpreted as Felipe Member (4.0 % K, 2.2 ppm U, 8.1 ppm Th).

## 6 Discussion

The island has been largely constructed as a shield volcano with fluid lava flows; however, some large explosive episodes have left their mark, with ignimbrite deposits exposed on different parts of the surface. An unusually large number of domes dot the flanks, the result of slow emplacement of largely degassed silicic magma, with extensive lava flows spreading from many of them and forming characteristic peninsulas around the island. Such a morphological feature is typical of peralkaline volcanoes (e.g., Pantelleria island; Orsi et al. 2008), and it is largely explained by the rheological behaviour of high-silica peralkaline magmas, that show a particularly low viscosity, between  $10^5$  and  $10^7$  Pa s at

750–850 °C (Stevenson and Wilson 1997), related to both peralkalinity and the abundance of chlorine and fluorine besides water (Neave et al. 2012). The occurrence of fast-moving lava flows on Socorro Island represents a potential source of relatively high volcanic hazard in case of renewed activity. Another potential source of extremely high volcanic hazard is related to the explosive character of many eruptions that have occurred on Socorro during its relatively recent volcanic history.

The caldera wall, first identified by Bryan (1966), has proved to be somewhat enigmatic. No evidence has been found to clearly associate a particular deposit with the formation of the caldera. Consequently it is not easy to define in clear terms the pre- and post-caldera rocks. Bryan (1966) first proposed that there was a quiescent period after the caldera-forming eruption, which he thought to be largely a collapse event with no significant explosive component. He further proposed that the majority of pre-caldera deposits consist of lava flows, whereby subsequent interpretations have identified them as ignimbrites (Carballido-Sanchez 1994; Bohrson et al. 1996), or more specifically as rheomorphic tuffs (Lower El Muerto Member), which are commonly confused with silicic lava flows (Orsi and Sheridan 1984). More recently, Sbarbori et al. (2009) report an absence of welding within the same deposits and propose this as evidence for the deposits not being ignimbrites, but instead were classified as lava flows interbedded with surge and ash deposits.

Given the small number of studies that have tried to decipher the geology of Isla Socorro, many questions remain open. Moreover, access to the island is very difficult over a large part of the island, with limited exposure of the deposits. Further difficulty is represented by the dense vegetation covering large areas (majority of the inland excluding the southeast).

Our high-resolution aeromagnetic data yielded an overall view of the island's magnetic features, regardless of the ruggedness and inaccessibility of many of its areas. We interpreted the wide minimum in the pole-reduced magnetic data as connected to a high-temperature zone (above the Curie temperature) in the deeper part of the volcano, consistently with temperatures of 500–600° C identified by previous studies (Taran et al. 2010). A *DEXP* analysis on upward continued magnetic data showed two large sources located around 5 km b.s.l. Based on what inferred in previous studies on magnetic field of volcanic islands (e.g., Napoli et al. 2007; Blanco-Montenegro et al. 2007) and on the depths found for the reservoirs of other peralkaline edifices (e.g., Lanzo et al. 2013), we relate these sources to feeding structures that are now filled with crystalline rocks. Our magnetic data also highlighted the possible existence of an ancient caldera rim located East of the known caldera wall (Bryan 1966). The presence of a newly detected caldera edge suggests the possibility that the island's caldera has a nested structure, similar to a number of other peralkaline edifices worldwide. Evidence of an older caldera structure helps to support the argument for the oldest pyroclastic deposits being ignimbrites rather than lava flows. Further mapping is required to fully determine the distribution of these deposits and confirm the nature of the eruptive history of the volcano.

In order to better assess the main compositional and alteration features of the Socorro terranes, a comparison has been made between the K, Th and U contents of volcanic rocks (data from Bohrson and Reid 1995, 1997) and the average contents determined by gamma-ray for the recognized volcanic members (Table 1). All data have been plotted in two binary diagrams K versus Th and K versus U (Fig. 8). The comparison shows several interesting features. First of all, geochemical data from the literature confirm the bimodality of Socorro volcanic rocks, with two dominant groups of mafic and silicic compositions showing good geochemical correlations. Secondly, the average K content of the recognized volcanic members is in the same range as that of the analysed volcanic



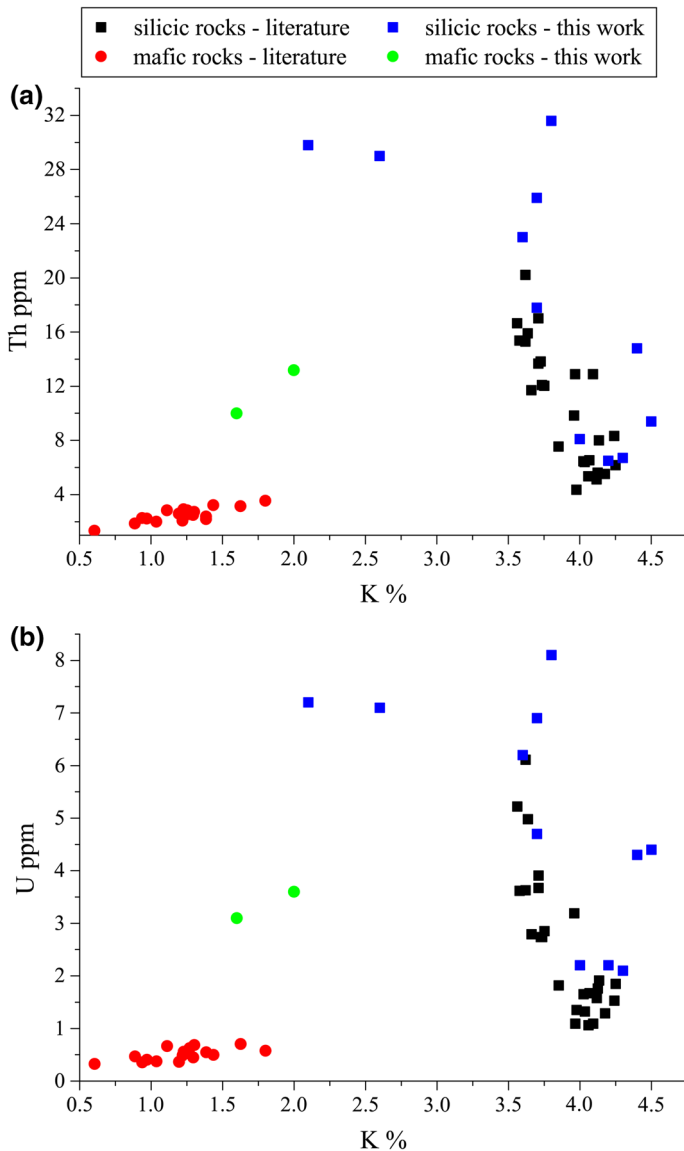


**Fig. 8** Binary diagrams of K % versus: **a** Th ppm, and **b** U ppm contents measured on volcanic rocks from Socorro Island (data from Bohrsen and Reid 1995, 1997), compared with K, Th and U average contents determined by gamma-ray for the recognized volcanic members (data from Table 1)

rocks, between ca. 0.5 and 4.5 %. Conversely, the average Th and U contents determined by gamma-ray survey are not exactly in the same range as those from the literature. The concentration range of both elements is shifted towards higher values. This might be caused by a bias in the gamma-ray technique relative to the analytical techniques used for the literature data (see Bohrsen and Reid 1995, 1997). Apart from that, two members display a clear depletion of potassium with respect to the literature data, which could be an

effect of rock alteration. They are El Bosque and Playa Norte members, among the oldest of Socorro, largely covering the northern and eastern sectors of the island. Thus, it is very likely that they have suffered a significant chemical weathering through time, also shown by their low K content in the map of Fig. 5. No other volcanic members display significant alteration features, nor any sign of U loss appears from this comparison; indeed, U and Th contents are well correlated. In summary, the comparison shows that, despite a significant analytical bias that introduces some uncertainty, the gamma-ray survey has been effective in identifying the main volcanic terranes cropping out on Socorro island, as well as allowing an evaluation of their alteration degree.

## 7 Conclusions

Through this work, we aimed at retrieving information about the surface and subsurface geology of the volcanic island of Socorro based on a new geologic survey (see Fig. 2) and on the analysis and interpretation of high-resolution magnetic and gamma-ray airborne data.

Our magnetic data (Fig. 4) yielded some new information about the structural setting of the island and its deep-seated magnetized structures (Fig. 6). No previous geophysical survey had ever been carried out aimed at investigating the deep structure of Socorro. The present work added new constraints to the previous knowledge on the deep structure of the island, which so far could only be inferred from the poor available geological and volcanological information.

The comparison between the revised geological map (Fig. 2) and the radiometric data (Fig. 5) has produced some interesting results (Fig. 7). This highlights the value of this technique when the geology is characterized by contrasting radioisotopic signatures. The present study demonstrates how useful the application of gamma-ray spectroscopy, integrated with geological data, can be for a site having remote location and difficult accessibility. This is especially crucial for active or dormant volcanoes that may represent a source of risk for exposed people in case of renewed activity. The exact shapes of the features in Fig. 7 were determined with the help of the satellite image of Socorro Island. Differences between the maps of Figs. 2 and 7 show areas where more fieldwork is necessary. Our radiometric results confirm the studies from Bohrson et al. (1996)—which were unfortunately confined to the Lomas Coloradas area—and partly disagree with the classification by Carballido-Sanchez (1994).

Differences between the geological and radiometric map could be explained by inaccuracies in the mapping or poor interpretation of aerial photographs. Moreover, two of the three considered radioelements, namely K and U, are fluid-mobile and thus sensitive to alteration. As a consequence, in some cases these differences might also be explained by a different alteration state of the members exposed at the surface.

Future fieldwork is required to remove some of the ambiguities and establish the most likely interpretation. Furthermore, a thorough geochemical characterization, including major, minor and trace elements of rock samples collected from the main volcanic deposits of the island, would add significant information about the true composition of the terranes, as well as their alteration state. An integrated evaluation of these with magnetic and gamma-ray airborne data would certainly help in a better understanding of the volcanic history of the island of Socorro, a critical step in establishing possible hazards on the island from any future volcanic activity.

**Acknowledgments** The authors are grateful to the Editor and two anonymous reviewers whose comments helped to improve the paper. They gratefully acknowledge the support of the Secretaría de Marina—Armada de México, and of Andreas Ahl, Geological Survey of Austria, for processing magnetic raw data. N.V. would like to thank the students from the Universidad de Colima and Colima Intercambio e Investigación en Volcanología who have participated in many trips to the island. This was partly funded by CONACYT Grant 41199-F.

## References

- Araña V, Camacho AG, García A, Montesinos FG, Blanco I, Vieira R, Felpeto A (2000) Internal structure of Tenerife (Canary Islands) based on gravity, aeromagnetic and volcanological data. *J Volcanol Geoth Res* 103(1–4):43–64
- Aydın I, Aydoğan MS, Oksum E, Kocak A (2006) An attempt to use aerial gamma-ray spectrometry results in petrochemical assessments of the volcanic and plutonic associations of Central Anatolia (Turkey). *Geophys J Int* 167(2):1044–1052
- Baker PE (1974) Peralkaline acid volcanic rocks of oceanic islands. *Bull Volc* 38:737–754
- Blanco-Montenegro I, De Ritis R, Chiappini M (2007) Imaging and modelling the subsurface structure of volcanic calderas with high-resolution aeromagnetic data at Vulcano (Aeolian Islands, Italy). *Bull Volc* 69(6):643–659
- Bohrson WA, Reid MR (1995) Petrogenesis of alkaline basalts from Socorro Island, Mexico: trace element evidence for contamination of ocean island basalt in the shallow ocean crust. *J Geophys Res* 100:24555–24576
- Bohrson WA, Reid MR (1997) Genesis of silicic peralkaline volcanic rocks in an ocean island setting by crustal melting and open-system processes: Socorro Island, Mexico. *J Petrol* 38:1137–1166
- Bohrson WA, Reid MR (1998) Genesis of evolved ocean island magmas by deep- and shallow-level basement recycling, Socorro Island, Mexico: constraints from Th and other isotope signatures. *J Petrol* 39:995–1008
- Bohrson WA, Reid MR, Grunder AL, Heizler MT, Harrison TM, Lee J (1996) Prolonged history of silicic peralkaline volcanism in the eastern Pacific Ocean. *J Geophys Res* 101:11457–11474
- Bryan WB (1966) History and mechanism of eruption of soda-rhyolite and alkali basalt, Socorro Island, Mexico. *Bull Volc* 29:453–480
- Carballido-Sanchez EA (1994) The geology and petrology of Socorro Island, Revillagigedo Archipelago, Mexico. PhD Thesis, Tulane University
- Cella F, Fedi M (2012) Inversion of potential field data using the structural index as weighting function rate decay. *Geophys Prospect* 60:313–336
- Chiozzi P, Pasquale V, Verdoya M (2009) Radiometric survey for exploration of hydrothermal alteration in a volcanic area. *J Geochem Explor* 93:13–20
- Civetta L, D’Antonio M, Orsi G, Tilton GR (1998) The geochemistry of volcanic rocks from Pantelleria Island, Sicily Channel: petrogenesis and characteristics of the mantle source region. *J Petrol* 39(8):1453–1491
- Cooper GRJ, Cowan DR (2006) Enhancing potential field data using filters based on the local phase. *Comput Geosci* 32:1585–1591
- Davis AS, Gunn SH, Bohrson WA, Gray L, Hein JR (1995) Chemically diverse, sporadic volcanism at seamounts offshore southern and Baja California. *GSA Bull* 107(5):554–570
- Di Carlo I, Rotolo SG, Scaillet B, Buccheri V, Pichavant M (2010) Phase equilibrium constraints on pre-eruptive conditions of recent felsic explosive volcanism at Pantelleria Island, Italy. *J Petrol* 51(11):2245–2276
- Farmer JD, Farmer MC, Berger R (1993) Radiocarbon ages of lacustrine deposits in volcanic sequences of The Lomas Coloradas area, Socorro Island, Mexico. *Radiocarbon* 35(2):253–262
- Fedi M (2007) DEXP: a fast method to determine the depth and the structural index of potential field sources. *Geophysics* 72:1–11
- Fedi M, Pilkington M (2012) Understanding imaging methods for potential field data. *Geophysics* 77(1):G13–G24
- Finn CA, Williams DL (1987) An aeromagnetic study of Mount St. Helens. *J Geophys Res* 92:10194–10206
- Finn CA, Sisson TW, Descsz-Pan M (2001) Aerogeophysical measurements of collapse-prone hydrothermally altered zones at Mount Rainier Volcano, Washington. *Nature* 409:600–603

- Finn CA, Deszcz-Pan M, Anderson ED, John DA (2007) Three-dimensional geophysical mapping of rock alteration and water content at Mount Adams, Washington, implications for lahar hazards. *J Geophys Res* 112:B10204
- Gehring I (2004) The use of grain-size dependent magnetic susceptibility and gamma-ray measurements for the detailed reconstruction of volcanostratigraphy: the case of La Fossa di Vulcano, S. Italy. *J Volcanol Geoth Res* 138:163–183
- Gioncada A, Landi P (2010) The pre-eruptive volatile contents of recent basaltic and pantelleritic magmas at Pantelleria (Italy). *J Volcanol Geoth Res* 189:191–201
- Grauch VJS, Cordell L (1987) Limitations of determining density or magnetic boundaries from the horizontal gradient of gravity or pseudogravity data. *Geophysics* 52:118–121
- Grauch VJS, Hudson MN, Minor SA (2001) Aeromagnetic expression of faults that offset basin fill, Albuquerque basin, New Mexico. *Geophysics* 66:707–720
- Hoovgard J, Grasty RL (1997) Reducing statistical noise in airborne gamma-ray data through spectral component analysis. In: Gubins AG (ed) *Proceedings of exploration 97, fourth decennial conference on mineral exploration*, pp 753–764
- IAEA (2003) Guidelines for radioelement mapping using gamma ray spectrometry data. International Atomic Energy Agency (IAEA), Nuclear Fuel Cycle and Materials Section, TECDOC 1363 Austria
- Ivan M (1994) Upward continuation of potential fields from a polyhedral surface. *Geophys Prospect* 42:391–404
- Kemski J, Klingel R, Siehl A (1996) Die terrestrische Strahlung durch natürliche radioaktive Elemente in Gesteinen und Böden. In: Siehl A (ed) *Extraction from "Umweltradioaktivität"*. Ernst & Sohn, Germany, pp 69–96
- Lanzo G, Landi P, Rotolo SG (2013) Volatiles in pantellerite magmas: a case study of the Green Tuff Plinian eruption (Island of Pantelleria, Italy). *J Volcanol Geoth Res* 262:153–163
- Lénat JF, Aubert M (1982) Structure of Piton de la Fournaise Volcano (La Reunion island, Indian Ocean) from magnetic investigations. An illustration of the analysis of magnetic data in a volcanic area. *J Volcanol Geoth Res* 12:361–392
- Macdonald R (1974) Nomenclature and petrochemistry of the peralkaline oversaturated extrusive rocks. *Bull Volc* 38:498–505
- Mahood GA (1984) Pyroclastic rocks and calderas associated with strongly peralkaline magmatism. *J Geophys Res* 89:8540–8552
- Mahood GA, Baker D (1986) Experimental constraints on depths of fractionation of mildly alkalic basalts and associated felsic rocks: Pantelleria, Strait of Sicily. *Contrib Miner Petrol* 93(2):251–264
- Mahood GA, Hildreth W (1983) Nested calderas and trapdoor uplift at Pantelleria, Strait of Sicily. *Geology* 11:722–726
- Mammerickx J, Naar DF, Tyce RL (1988) The mathematician paleoplate. *J Geophys Res* 93(B4):3025–3040
- Mastellone D, Fedi M, Ialongo S, Paoletti V (2014) Volume upward continuation of potential fields from the minimum-length solution: an optimal tool for continuation through general surfaces. *J Appl Geophys* 111:346–355. doi:10.1016/j.jappgeo.2014.10.020
- Moore JG (1970) Submarine basalt from the Revillagigedo Islands, Region, Mexico. *Mar Geol* 9:331–345
- Motschka K (2001) Aerogeophysics in Austria. *Bull Geol Surv Jpn* 2(3):83–88
- Nabighian MN, Grauch VJS, Hansen RO, LaFehr TR, Li Y, Peirce JW, Phillips JD, Ruder ME (2005) The historical development of the magnetic method in exploration. *Geophysics* 70:33ND–61ND
- Napoli R, Currenti G, Del Negro C (2007) Internal structure of Ustica volcanic complex (Italy) based on a 3D inversion of magnetic data. *Bull Volc* 69(8):869–879
- Neave DA, Fabbro G, Herd RA, Petrone CM, Edmonds M (2012) Melting, differentiation and degassing at the Pantelleria volcano, Italy. *J Petrol* 53(3):637–663
- Orsi G, Sheridan MF (1984) The Green Tuff of Pantelleria: rheoignimbrite or rheomorphic fall? *Bull Volc* 47:611–626
- Orsi G, Civetta L, D'Antonio M, Carandente A (2008) L'isola di Pantelleria: un vulcano pantelleritico attivo nel Rift del Canale di Sicilia. *Geol Sicil Boll Ordine Reg Geol Sicil XVI*(3):5–12
- Paoletti V, Pinto A (2005) Aeromagnetic and radiometric data localized filtering at the Vesuvian Volcanic Area. *Boll Geofis Teor Appl* 46(2–3):245–259
- Paoletti V, Secomandi M, Florio G, Fedi M, Rapolla A (2005a) The integration of remote sensing magnetic data in the Neapolitan volcanic district. *Geosphere* 1(2):85–96
- Paoletti V, Supper R, Chiappini M, Fedi M, Florio G, Rapolla A (2005b) Aeromagnetic survey of the Somma-Vesuvius volcanic Area. *Ann Geophys* 48(2):199–213
- Paoletti V, Ialongo S, Florio G, Fedi M, Cella F (2013) Self-constrained inversion of potential fields. *Geophys J Int* 195(2):854–869

- Pilkington M, Keating P (2004) Contact mapping from gridded magnetic data—a comparison of techniques. *Explor Geophys* 35:306–311
- Roest WR, Verhoef J, Pilkington M (1992) Magnetic interpretation using the 3-D analytic signal. *Geophysics* 57:116–125
- Rollin P, Cassidy J, Locke CA, Rymer H (2000) Evolution of the magmatic plumbing system at Mt Etna: new evidence from gravity and magnetic data. *Terra Nova* 12(5):193–198
- Sbarbori E, Tauxe L, Goguitchaichvili A, Urrutia-Fucugauchi J, Bohron WA (2009) Paleomagnetic behavior of volcanic rocks from Isla Socorro, Mexico. *Earth Planets Space* 61:191–204
- Siebe C, Komorowski JC, Navarro C, McHone J, Delgado H, Cortes A (1995) Submarine eruption near Socorro Island, Mexico: geochemistry and scanning electron microscopy studies of floating scoria and reticulite. *J Volcanol Geoth Res* 68:239–271
- Skácelová Z, Rapprich V, Mlčoch B (2009) Effect of small potassium-rich dykes on regional gamma-spectrometry image of a potassium-poor volcanic complex: a case from the Doupovské hory Volcanic Complex, NW Czech Republic. *J Volcanol Geoth Res* 187(1–2):26–32
- Stevenson RJ, Wilson L (1997) Physical volcanology and eruption dynamics of peralkaline agglutinates from Pantelleria. *J Volcanol Geoth Res* 79:97–122
- Taran YA, Fischer TP, Cienfuegos E, Morales P (2002) Geochemistry of hydrothermal fluids from an intraplate ocean island: everman volcano, Socorro Island, Mexico. *Chem Geol* 188:51–63
- Taran YA, Varley NR, Inguaggiato S, Cienfuegos E (2010) Geochemistry of H<sub>2</sub>- and CH<sub>4</sub>-enriched hydrothermal fluids of Socorro Island, Revillagigedo Archipelago, Mexico. Evidence for serpentinization and abiogenic methane. *Geofluids* 10:542–555
- Valenzuela RW, Galindo M, Pacheco JF, Iglesias A, Terán LF, Barreda JL, Coba C (2005) Seismic survey in southeastern Socorro Island: background noise measurements, seismic events, and T phases. *Geofís Int* 44:23–38
- Varley NR, Sandberg S, MacNeil R, Wooller L (2004) Integrated study of a volcanic hydrothermal system: Isla Socorro, Mexico. IAVCEI General Assembly, Pucón, pp 15–19
- Verduzco B, Fairhead JD, Green CM (2004) New insights into magnetic derivatives for structural mapping. *Lead Edge* 23(2):116–119